

# Using GEOBIA for Feature Extraction from Multitemporal SAR Images: Preliminary Results

Donato Amitrano\*, Francesca Cecinati<sup>†</sup>, Gerardo Di Martino\*, Antonio Iodice\*,  
Pierre-Philippe Mathieu<sup>‡</sup>, Daniele Riccio\* and Giuseppe Ruello\*

\*Department of Electrical Engineering and Information Technology

University of Napoli Federico II, Napoli, Italy

<sup>†</sup>Department of Civil Engineering

University of Bristol, Bristol, UK

<sup>‡</sup>European Space Agency

ESA ESRIN, Frascati, Italy

**Abstract**—In this paper, we explore the possibility to exploit GEOBIA concepts for extracting features from multitemporal SAR images. The proposed processing chain is feed by the recently introduced products of the Level-1 $\alpha$  and Level-1 $\beta$  families and aims at providing an unsupervised tool for information extraction particularly oriented toward the end-user community. The principal characteristics and the effectiveness of the framework are illustrated through two examples concerning urban area mapping and small reservoir extraction in semiarid environment.

## I. INTRODUCTION

Today, several sensors orbit around the Earth providing data throughout the whole electromagnetic allowing for the building of a better knowledge of the world we live. Remote sensing involves a large variety of professionals with different expertise and background. Therefore, when a processing chain is designed, it is highly desirable that it takes into account that its potential user could belong to the end-user or decision maker communities, in which it is widespread the use of GIS tools.

In this paper, we propose a new framework whose purpose is to mix classic multitemporal SAR processing and GEOBIA to provide to end-user a robust tool for unsupervised information extraction. The general flowchart we design is depicted in Fig. 1. The starting point is SAR time series, which is treated with multitemporal processing for the generation of a product of the Level-1 $\alpha$  [1] or of the Level-1 $\beta$  [2] family. This image is treated with self-organizing map (SOM) clustering [3] to segment the image in meaningful regions basing on color homogeneity. A basic semantic (constituted by a color label) is attached to each cluster, and it is exploited to initialize the object-based image analysis for feature extraction.

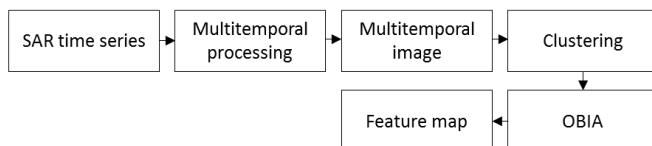


Fig. 1: Proposed processing chain.

The work is organized as follows. In Section II, the main characteristics of the RGB products are briefly discussed through examples. Applications exploiting the proposed framework are addressed in Section III. Conclusions are drawn at the end of the work.

## II. RGB PRODUCTS

In this Section, we briefly recall the characteristic of the input multitemporal RGB products. More information about the relevant processing chains can be found in [1], [2].

### A. Level-1 $\alpha$ products

Level-1 $\alpha$  products are bi-temporal images particularly oriented toward change-detection applications. They combine two intensity images, while the third channel is reserved to the interferometric coherence (it is useful for the identification of man-made targets, which are stable with respect to phase). One of the intensity images plays the role of the reference situation, i.e. the condition with respect changes are evaluated.

The following example is useful to clarify the main characteristics of these products. We consider a semiarid environment in Burkina Faso (western Africa). In this area, the climate is characterized by a long dry season (at the end of which the landscape is almost completely dry), and by a short and intense wet season, in which a lot of vegetation is expected on the scene.

The product depicted in Fig. 2 is composed as follows. On the blue band we loaded an image acquired at the peak of the dry season. It represents the reference image. On the green band, an image acquired during the wet season is placed. We will refer to it as test image, representing the acquisition in which the analyst wants to evaluate the changes in the land cover. This composition leads to the following interpretation of the displayed colors [1]:

- A balance between the blue and green channels identify unchanged land cover. Bare soil is rendered in a cyan tonality. Permanent surface water is displayed in black;
- The green color identifies a change in the land cover of the test image. In this case, it can be identified with

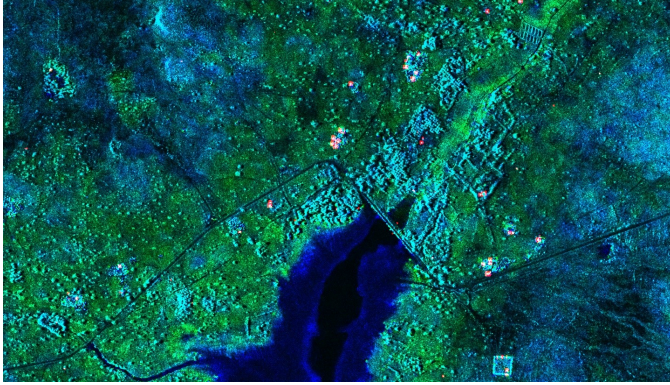


Fig. 2: Burkina Faso, Level-1 $\alpha$  product. Blue band: dry season image. Green band: wet season image. This combination allows for rendering in natural colors water and vegetation. The red band is reserved to the interferometric coherence. It is useful to identify small human settlements.

growing vegetation due to volumetric enhancement of backscattering [4];

- The blue color represents temporary surface water, i.e. areas covered by water during the acquisition of the test image (wet season). In fact, in this case, the terrain backscattering of the dry season image (blue band, reference image) is dominant;
- Bright targets identify small settlements due to the high contribution of both intensity and coherence channels. In fact, when images acquired with high temporal baseline are considered, only stable targets are expected to exhibit a high interferometric coherence.

This composition allows for rendering in natural colors the most important features of the study area, i.e. water and vegetation.

An important property of Level-1 $\alpha$  imagery is the stability with respect to variation of the scene and/or of the climatic conditions. In other words, if the scene is completely changed, the association color-object is the RGB product is the same [1].

### B. Level-1 $\beta$ products

Level-1 $\beta$  products are obtained by the fusion a time-series in an unique RGB frame [2]. These products are particularly oriented toward classification applications. In fact, they are composed by temporal features allowing for the identification of different features basing on their time dynamics. As for Level-1 $\alpha$  imagery, the objective is to provide an image with a consistent rendering of information, in which the association color-feature is physical-based and stable.

In Fig. 3, a sample Level-1 $\beta$  product is provided. It concerns the city of Castel Volturno (Southern Italy). The product composition is the following: on the red band the time series variance is loaded; on the green band the mean intensity is displayed; on the blue band a combination of the saturation index (it is proportional to the maximum span in backscattered energy) and of the interferometric coherence is placed. In

particular, the coherence is used when its value is above a user-defined threshold. It is useful to separate the built-up feature from highly variable natural targets.



Fig. 3: Castel Volturno (Italy): Level-1 $\beta$  product composed by six images belonging to the summer season of the year 2010. Product composition: red band - time series variance; green band - time series mean; blue band: combination of saturation index and mean interferometric coherence.

Given the aforementioned product composition, the following association color-object can be made 2:

- The sea surface is displayed in blue due to the Bragg scattering causing a significant contribution of the saturation index;
- Unchanged land cover is rendered in green due to the dominance of the mean band;
- The built-up feature is displayed in cyan due to the contributions of the interferometric coherence and of the mean intensity;
- Growing crops are displayed in yellow or pink due to a significant contribution of the variance and/or of the saturation index, depending on the kind of cultivation.

## III. APPLICATIONS

In this Section, we will show how to adapt the general diagram depicted in Fig. 1 to two different remote sensing problems, i.e. the urban area mapping and the small reservoirs extraction in semi-arid environment.

### A. Small reservoirs extraction in semiarid environment

In semiarid environment, small reservoirs are a fundamental resource for to face water scarcity during the long periods of drought. Therefore, their monitoring is crucial for the wellness of local population. In this context, remote sensing technologies can be very helpful, providing up-to-date information with high temporal frequency in areas which would be otherwise scarcely monitored [5].

To address this problem, the general schema depicted in Fig. 1 is adapted as follows (see Fig. 4: the product treated with SOM clustering is used to define a dictionary relevant with the feature. This dictionary is used to build a pre-classification mask representing the input for the calculation of two object layers, one scattering-based, the other geometry-based. The

scattering layer is given by the mean (computed object-wise) of the seasonal water pseudo-probability (SWPP) [6], which is computed as follows:

$$\text{SWPP} = \left[ 1 - \left( \frac{G}{255} \right)^2 \right] \frac{B - G}{B + G}, \quad \text{SWPP} \in [-1, 1]. \quad (1)$$

In this formula,  $B$  and  $G$  are the blue and the green band of a Level-1 $\alpha$  product, respectively. Roughly, this formulation allows for having a high response in areas appearing in blue color in the RGB product. For further details, the reader can refer to [6].

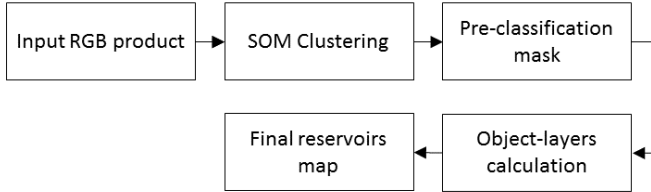


Fig. 4: Object-based image analysis chain adapted to the case of small reservoirs mapping.

The geometric layer is represented by the candidate objects' compactness, which is computed as follows [7]:

$$C = \frac{4\pi A}{P^2}, \quad C \in ]0, 1]. \quad (2)$$

In this formula,  $A$  and  $P$  represent objects' area and perimeter, respectively.

Objects having the scattering and geometric properties which are likely to be those of a reservoir (high SWPP and high compactness) are selected through a fuzzy system [8], allowing for the building of the final reservoirs map.

In TABLE I, we compared the results obtained using the proposed framework with those given by some simple pixel-based supervised classifiers. In particular, a SWPP-based reservoirs extraction [6] and a maximum likelihood (ML)-based reservoirs extraction were tested.

TABLE I: Small reservoirs extraction, comparison between the proposed object-based unsupervised extraction with some pixel-based classifiers. SWPP: seasonal water pseudo-probability. ML: maximum-likelihood.  $T$ : number of clusters or applied threshold, OA: overall accuracy, FA: false alarm rate.

Date	Method	$T$	OA (%)	FA $\times E^{-4}$
31/08/2010	Proposed	25	84.6	0.52
	SWPP	0.3	89.8	1.35
	ML	na	89.3	0.95
05/10/2014	Proposed	25	86.1	1.38
	SWPP	0.3	90.2	1.60
	ML	na	96.6	2.96

From this Table, it arises that the proposed (unsupervised) object-based framework allows for reducing significantly the

false alarm rate. Conversely, as expected, pixel-based method allow for reaching a higher overall accuracy.

Here we used 25 number of clusters to test the performance of our method. Further experiments are ongoing to test the effect of the variation of this parameter on the overall performance of the method.

### B. Urban area mapping

The block diagram of the proposed algorithm for urban area mapping is shown in Fig. 5. The input product is, as aforementioned, a RGB image of the Level-1 $\alpha$  or Level-1 $\beta$  family. As for reservoirs extraction, this product is treated with SOM clustering [3] for dimensionality reduction. The semantic color label attached to each cluster is exploited to initialize the OBIA. In particular, the clusters relevant with the built-up environment are selected through the definition of a dictionary, and this represents the coarse urban area map which is then refined to build the final urban area map. In fact, the OBIA has the purpose to connect sparse built-up objects identified in the coarse map, avoiding an unreliable fragmentation of the retrieved urban area through simple spatial reasoning [9]. Operatively, with respect to the small reservoirs case, now the OBIA is simpler, since its purpose is to fill the "holes" which are typical of the urban area maps produced using pixel-based methods. In fact, the feature which is usually exploited in SAR imagery as driver of the urban area is the built-up, which is often very scattered over the scene, especially when the urban areas are not dense. Moreover, objects allows for a more effective modeling of the urban-rural gradient, ensuring a reliable mapping of the spreading of the urban land into the surrounding natural landscape [10].

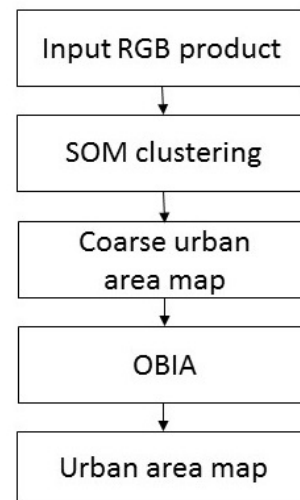


Fig. 5: Processing chain for urban area mapping.

The output of the proposed algorithm is a map with different levels of urban density. An example, concerning a densely populated area in Southern Italy in the nearby of the city of Naples, is shown in Fig. 6. In particular, in Fig. 6a, the RGB product used as input of the whole processing is shown. The

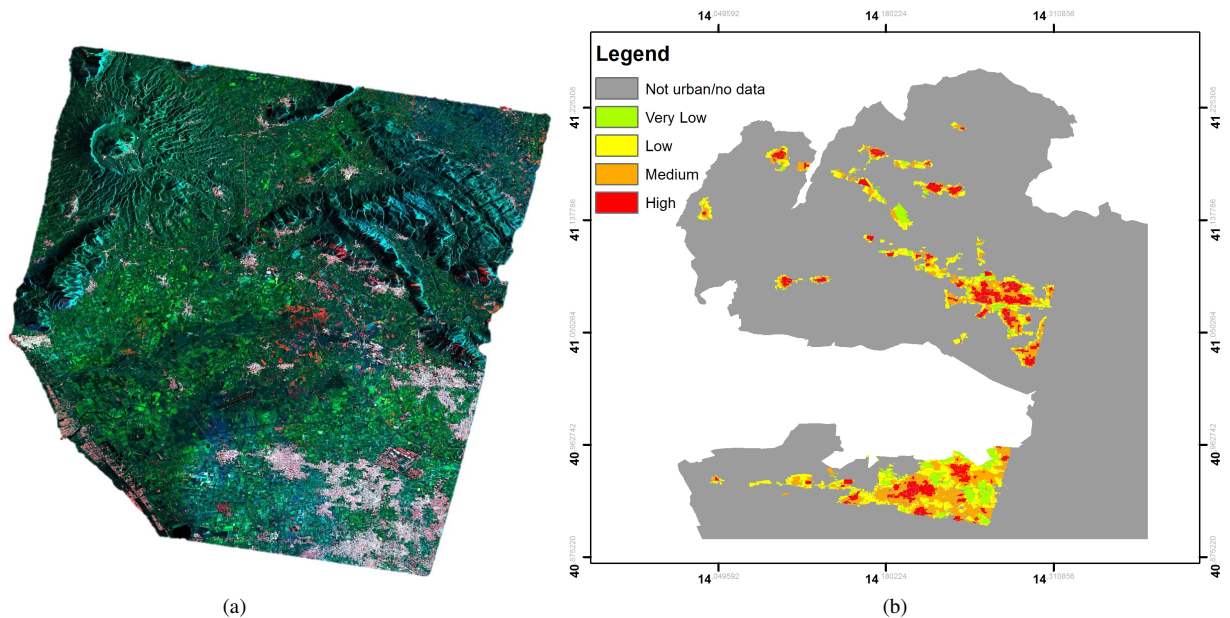


Fig. 6: Urban area mapping using the proposed object-based processing. The case study concerns a densely populated area in the nearby of the city of Naples. (a) Input RGB Level-1 $\alpha$  product derived from COSMO-SkyMed data with 15 meters spatial resolution. (b) Output urban area map with five levels of urban density re-projected into the Urban Atlas grid.

urban area is represented in white. In Fig. 6b, the output urban area map with five level of built-up density is depicted. It has been re-projected into the Urban Atlas grid. To each polygon in the reference map, the SAR class with the higher number of occurrence (computed pixel-based) has been assigned.

At visual level, a good agreement between the two products can be observed. Quantitatively, the accuracy of the obtained product was measured through comparison with a Urban Atlas derived ground truth in a urban/not urban classification. The result of this comparison was quite satisfying, since we found an agreement of about 90% for the considered case study.

#### IV. CONCLUSIONS

In this paper, we presented a new framework for unsupervised feature extraction from multitemporal SAR images. The input products are represented by RGB images of the Level-1 $\alpha$  or Level-1 $\beta$  family, which are, as first, treated with self-organizing map clustering for dimensionality reduction. In the same time, a basic verbal attribute referring to clusters' color is attached to each image segment. This color attribute is used to build a pre-classification mask, which is then processed with a application-oriented OBIA for information extraction.

Two applications exploiting the proposed framework have been discussed, each one having a different OBIA. The first one was small reservoirs mapping in semi-arid environment. In this case, the proposed object-based framework allowed for a significant reduction of the false alarm rate with respect to pixel-based techniques, keeping a high overall accuracy. The second application was about urban area mapping, in which the reasoning through objects allowed for solving the problems related with the fragmentation of the urban environment typical of pixel-based methods.

The proposed framework, mixing classic SAR processing and GEOBIA concepts, aims at providing a easy-to-use unsupervised tool for end-users.

#### REFERENCES

- [1] D. Amitrano, G. Di Martino, A. Iodice, D. Riccio, and G. Ruello, "A New Framework for SAR Multitemporal Data RGB Representation: Rationale and Products," *IEEE Trans. Geosci. Remote Sens.*, vol. 53, no. 1, pp. 117–133, 2015.
- [2] D. Amitrano, F. Cecinati, G. Di Martino, A. Iodice, P.-P. Mathieu, D. Riccio, and G. Ruello, "Multitemporal Level-1 $\beta$  Products: Definitions, Interpretation, and Applications," *IEEE Trans. Geosci. Remote Sens.*, vol. 54, no. 11, pp. 6545–6562, 2016.
- [3] T. Kohonen, *Self-Organizing Maps*. Berlin, Heidelberg: Springer-Verlag, 2001.
- [4] A. K. Fung, "Scattering from a Vegetation Layer," *IEEE Trans. Geosci. Elect.*, vol. 17, no. 1, pp. 1–6, 1979.
- [5] D. Amitrano, F. Ciervo, G. Di Martino, M. N. Papa, A. Iodice, Y. Kousoubé, F. Mitidieri, D. Riccio, and G. Ruello, "Modeling Watershed Response in Semiarid Regions with High Resolution Synthetic Aperture Radars," *IEEE J. Sel. Topics Appl. Earth Observ.*, vol. 7, no. 7, pp. 2732–2745, 2014.
- [6] D. Amitrano, G. Di Martino, A. Iodice, D. Riccio, and G. Ruello, "Small Reservoirs Extraction in Semi-Arid Regions Using Multitemporal Synthetic Aperture Radar Images," *IEEE J. Sel. Topics Appl. Earth Observ.*, In press.
- [7] E. P. Cox, "A method of assigning numerical and percentage values to the degree of roundness," *J. Paleontol.*, vol. 1, no. 3, pp. 179–183, 1927.
- [8] D. Amitrano, V. Belfiore, F. Cecinati, G. Di Martino, A. Iodice, P.-P. Mathieu, S. Medagli, D. Poreh, D. Riccio, and G. Ruello, "Urban Areas Enhancement in Multitemporal SAR RGB Images Using Adaptive Coherence Window and Texture Information," *IEEE J. Sel. Topics Appl. Earth Observ.*, vol. 9, no. 8, pp. 3740–3752, 2016.
- [9] D. Amitrano, F. Cecinati, G. Di Martino, A. Iodice, P.-P. Mathieu, D. Riccio, and G. Ruello, "Multitemporal Synthetic Aperture Radar for Urban Planning and Critical Infrastructure Monitoring," in *IEEE Joint Urban Remote Sensing Event*, 2015.
- [10] J. R. Weeks, "Defining Urban Areas," in *Remote Sensing of Urban and Suburban Areas*, T. Rashed and C. Jürgens, Eds. Berlin: Springer, 2010.